Chemical Science

ROYAL SOCIETY OF CHEMISTRY

REVIEW

View Article Online
View Journal | View Issue

Cite this: *Chem. Sci.*, 2022, **13**, 329

Materials by design at high pressures

Meiling Xu, [a] Yinwei Li *[a] and Yanming Ma *[bc]

Pressure, a fundamental thermodynamic variable, can generate two essential effects on materials. First, pressure can create new high-pressure phases *via* modification of the potential energy surface. Second, pressure can produce new compounds with unconventional stoichiometries *via* modification of the compositional landscape. These new phases or compounds often exhibit exotic physical and chemical properties that are inaccessible at ambient pressure. Recent studies have established a broad scope for developing materials with specific desired properties under high pressure. Crystal structure prediction methods and first-principles calculations can be used to design materials and thus guide subsequent synthesis plans prior to any experimental work. A key example is the recent theory-initiated discovery of the record-breaking high-temperature superhydride superconductors H_3S and LaH_{10} with critical temperatures of 200 K and 260 K, respectively. This work summarizes and discusses recent progress in the theory-oriented discovery of new materials under high pressure, including hydrogen-rich superconductors, high-energy-density materials, inorganic electrides, and noble gas compounds. The discovery of the considered compounds involved substantial theoretical contributions. We address future challenges facing the design of materials at high pressure and provide perspectives on research directions with significant potential for future discoveries.

Received 3rd August 2021
Accepted 8th December 2021

DOI: 10.1039/d1sc04239d

rsc.li/chemical-science

1 Introduction

Pressure, a fundamental thermodynamic variable, can dramatically reduce interatomic distances and alter chemical bonds to induce structural transformations and new high-pressure phases.[1,2] In general, each material is expected to experience several structural transformations when compressed up to a pressure of a million atmospheres. Additionally, new oxidation states appearing under high pressure can stabilize new compounds with unconventional stoichiometries.[3–7] As an example, we can consider the unconventional Na_3Cl and $NaCl_3$ stoichiometries of Na and Cl that form under pressure rather than the known chemical species NaCl.[8] These new high-pressure phases and compounds often exhibit exotic physical and chemical properties and are thus potentially functional materials. Pressure is therefore an efficient tool in developing new materials that are inaccessible at ambient pressure.

Since the first achievement of lab pressure at ~10 GPa in a so-called large-volume apparatus obtained by Percy Bridgeman in 1905, many high-pressure generating techniques have been developed.[9–12] This includes the static-pressure generating equipment such as diamond anvil cells (DAC) and large-volume presses (multiple-anvil system, piston-cylinder devices and sealed vessel systems), and large-scale shock-wave facilities that generate dynamic compression. DAC is the most widely used device to generate steady-state pressure with a record upper pressure of above 1000 GPa (ref. 12) achieved by using nano-diamonds as second-stage anvils in double-stage DAC, much higher than that (~30 GPa (ref. 13)) generated by large-volume presses. Dynamic-compression facilities could generate pressures well above terapascal by using shock waves produced by gas guns, laser-driven compression or hemispherically converging explosives, capable of reaching 5000 GPa on a ~1 mm^3 sample for a fraction of a second.[13] The fairly high upper frontiers of pressure expanded tremendously the searching space for new functional materials.

Exploration of new materials often involves experimental trial and error, with a range of possible compounds being synthesized and compared to identify the best. This is a time-consuming and expensive process. A classic example is Edison's testing of approximately 8000 materials over two years to find a material durable enough to provide electric lighting for 1000 hours. An experimental search for target functional materials among the large number of new phases and unconventional compounds available under high pressure would be challenging. Considering hydrides as an example, little experimental progress in these potential high-temperature superconductors was made before 2014 due to the great variety of hydrides at high pressure. Only when theoretical work explicitly identified highly compressed H_2S as a superconductor,[14] the

[a]*Laboratory of Quantum Functional Materials Design and Application, School of Physics and Electronic Engineering, Jiangsu Normal University, Xuzhou 221116, China. E-mail: yinwei_li@jsnu.edu.cn*

[b]*State Key Laboratory of Superhard Materials & International Center for Computational Method and Software, College of Physics, Jilin University, Changchun 130012, China. E-mail: mym@jlu.edu.cn*

[c]*International Center of Future Science, Jilin University, Changchun 130012, China*

H_3S superconductor with a critical temperature (T_c) of 200 K was subsequently developed.[15] This demonstrates the successes possible when theoretical and experimental efforts are applied together to the discovery of new materials at high pressure.

Developments in crystal structure prediction (CSP) and first-principles calculations have improved the accuracy of the prediction of the structures and properties of new phases and unconventional compounds formed at high pressure, thus prompting the discovery of new materials by design.[15–20] Unbiased CSP methods without any experimental input can predict the energetically most stable or metastable structures at a given pressure, leading to the construction of the phase diagram of a considered system. First-principles calculations can simulate the mechanical, thermal, optical, electronic, and magnetic properties of these high-pressure unconventional compounds and the pressure and temperature conditions for their synthesis, thus allowing theoretical findings to guide the choice of experiments attempted. In 2011, the U.S.A., Japan, and China successively announced the Materials Genome Projects, aiming to combine theory and experiment to accelerate the development of new materials.

Theoretical design for high-pressure synthesis has aided several major experimental discoveries of new materials. A milestone example is the theory-initiated discovery of the record-breaking high-temperature superconductors H_3S[14,15,21] and LaH_{10} (ref. 6, 7, 22 and 23) with T_c values of 200 K and 260 K, respectively. Other discoveries include high-energy-density materials (*e.g.*, cg-N,[24,25] layered *Pba*2 polymeric nitrogen,[26] and LiN_5 (ref. 27)), inorganic electrides (*e.g.*, Na,[16] Ca_2N,[28] and Sr_5P_3 (ref. 29)), and noble gas compounds (*e.g.*, $XeFe_3$,[4] $XeNi_3$,[4] Na_2He,[5] and Xe_3O_2 (ref. 30)).

This review surveys these materials, with particular emphasis on their theory-oriented discovery at high pressure. First, we highlight the effect of pressure on materials and discuss the stabilization of new materials. Second, the theoretical methods for material design, especially CSP methods, are discussed. Third, we summarize and discuss recent discoveries of materials at high pressure initiated by theoretical design. We particularly focus on hydrogen-rich superconductors, high-energy-density materials, inorganic electrides, and noble gas compounds. Our work concludes with descriptions of the main drawbacks of high-pressure materials and a discussion of the possible solutions and future research directions. Actually, these available reviews[1,2,31–33] either focus on new materials with a given function such as superconductivity, or summarize all designed materials at high pressure. Here, our review intends to summarize those materials discovery initiated by theoretical design at high pressure, with a purpose to highlight the leading role of structure prediction in material discovery.

2 Effect of pressure on materials

High pressure provides two main routes to stabilize new materials. First, the decrease in the interatomic distance under compression redistributes valence electrons and alters bonding patterns, thereby effectively modulating the relative energetic stability of possible structures on the potential energy surface and generating new high-pressure phases *via* structural transformations. A typical example is the pressure-induced phase transformation of sp^2-hybrid graphite to sp^3-hybrid diamond.[34] Pressure helps overcome the energy barrier for the conversion between the two carbon phases, making diamond the global energy minimum. Each element or compound undergoes several structural transformations at high pressure. For example, at least six phase transformations have been observed or predicted for the alkali metal Na (bcc → fcc (65 GPa) → cI16 (103 GPa) → tI19 (156 GPa) → hP4 (200 GPa) → oP8 (1.75 TPa) → cI24 (>15.5 TPa)),[16,35] among which the transformation into the transparent hP4 phase is particularly interesting as it characterizes a so called anti-Wilson transition, *i.e.*, transformation of a good metal into an insulator, that violates the traditional wisdom of Wilson transition.[16] Many high-pressure phases with exotic properties have been discovered with potential applications, including superconducting phases (*e.g.*, H_2S[14] and AlH_3 (ref. 36)), polymeric nitrogen (*e.g.*, cg-N,[24,25] LP-*Pba*2 (ref. 26) and LP-N[37]), and electrides (*e.g.*, Li[38] and Na[16,35]).

Pressure can also stabilize compounds and phases by reordering the energies of outer atomic orbitals, causing charge transfer between different orbitals, thus modifying the chemical identity of atoms *via* the appearance of new oxidation states and leading to the formation of unconventional compounds that are inaccessible at ambient pressure. For example, the alkali metal Cs shows oxidation states of +3 and +5 at high pressure rather than the +1 state observed at ambient pressure, as evidenced by the unconventional CsF_3 and CsF_5 compounds predicted at high pressure in addition to the typical CsF[39] known at ambient pressure. Another example is the formation of compounds of the inert element Xe. Its fully occupied 5p valence states can be partially excited to unoccupied orbitals at high pressure, activating the Xe 5p electrons to form compounds such as $XeFe_3$.[4] Advanced structure prediction methods have predicted various unconventional compounds formed at high pressure that have since been experimentally confirmed, including high-T_c superconducting hydrides (*e.g.*, H_3S,[14,15,21] LaH_{10},[6,7] YH_6,[40] and C–S–H[41,42]), high-energy-density nitrogen-rich compounds (*e.g.*, LiN_5 (ref. 27) and CsN_5 (ref. 43)), electrides (*e.g.*, Sr_5P_3 (ref. 29) and Na_2He[5]), and noble gas compounds (*e.g.*, $XeFe_3$,[4] $XeFe_5$,[4] and Na_2He[5]).

3 Theoretical methods for material design

The crystal structure is one of the most fundamental pieces of information needed to characterize a material. Its prediction for a given compound at high pressures without any prior information is therefore a primary task in material design. This is now possible due to the development of CSP methods such as Crystal structure AnaLYsis by Particle Swarm Optimization (CALYPSO) (based on particle swarm optimization[44,45]), *ab initio* random structure searching (AIRSS) (based on random sampling[46]), Universal Structure Predictor: Evolutionary Xtallography (USPEX) (based on a genetic algorithm[47]), Xtallography

Optimization (XtalOpt),[48] Global Space-Group Optimization (GSGO),[49] and Evolutionary Algorithm (EVO).[50]

These methods have been proven efficient in identifying the global energy minimum among the vast number of local minima on the potential energy surface, making them powerful tools for materials by design.[51–61] Consider, for example, a binary system formed by elements A and B; material-by-design research requires construction of a convex hull map of composition *vs.* formation enthalpy to screen the thermodynamically most stable stoichiometries. This can be achieved *via* systematic structure predictions of candidate A_xB_y stoichiometries at selected pressures through the combination of CSP and first-principles calculations. Once the most stable structure of each A_xB_y is obtained, a formation enthalpy *vs.* composition convex hull can be constructed to screen out the thermodynamically stable compounds. The convex hull presents also the possible precursors to synthesize the candidate stable compounds, providing essential information to guide the subsequent experiments. Finally, the useful properties (*e.g.*, electronic band structure, phonons, and electron-phonon coupling parameters, *etc.*) of the stable compound can be simulated by performing first-principle calculations.

4 Theory-oriented discovery of pressure-induced materials

Here, we summarize and discuss recent accomplishments in material discovery at high pressure initiated by theoretical design. These materials include hydrogen-rich superconductors, high-energy-density materials, inorganic electrides, and noble gas compounds.

4.1 Hydrogen-rich superconductors

Room-temperature superconductivity is the holy grail of condensed-matter physics. Before 2014, there is no report on

Table 1 Examples of theory-initiated discovery of hydrogen-rich superconductors under high pressures

Materials	Brief description	Year	References
H–S	The first theoretical prediction of H_2S with 80 K superconductivity at 160 GPa	2014 (September)	14
	Theoretical prediction of H_3S with ~200 K superconductivity at 200 GPa	2014 (November)	21
	Experimental confirmation of the superconductivity in compressed H_2S and the observation of the record 203 K superconductivity	2015	15
	Experimental confirmation of the pressure-driven disproportionation of H_2S to H_3S, contributing the 203 K superconductivity	2016	66 and 69
C–S–H	Theoretical prediction of a metastable CSH_7 with 190 K superconductivity at 150 GPa	2021 (April)	42
	Theoretical prediction of a metastable CSH_7 with 181 K superconductivity at 100 GPa	2021 (May)	41
	Experimental synthesis of CSH_x with 288 K superconductivity at 267 GPa	2021 (October)	20
LaH_{10}	Theoretical prediction of LaH_{10} with 255–288 K superconductivity at 250 GPa	2017	6 and 7
	Experimental observation of superconductivity at 260 K in LaH_{10} by compressing La and hydrogen at 200 GPa	2019 (January)	22
	Experimental observation of superconductivity at 250 K in LaH_{10} by compressing NH_3BH_3 and La at 170 GPa	2019 (May)	23
CaH_6	The first predicted clathrate hydride with superconductivity of 235 K at 150 GPa	2012	79
	Experimental synthesis of CaH_6 with 215 K superconductivity at 172 GPa	2021	81

the T_c values that have ever exceeded 40 K for conventional superconductors. Hydrogen-rich compounds at high pressure have long been sought as high T_c superconductors.[62] However, the large amount of unknown hydrogen-containing compounds that can possibly exist under high pressure poses a great challenge to experimentalists seeking candidate hydrides to test. Little progress was initially made experimentally, but theoretical designs of hydrogen-rich superconductors by the aid of CSP methods have led to a series of experimental breakthroughs. The two main categories of superconducting hydrides discovered thus far are the covalent H_3S and the ionic clathrate structured, the superconductivity of which arises mainly through S–H covalent bonds and caged H sublattices with encaged metals, respectively (Table 1).

4.1.1 Covalent hydrides. The first breakthrough in this field was the observation by Drozdov *et al.* of remarkable high-temperature superconductivity (T_c = 203 K) in compressed H_2S.[15] This was inspired by a theoretical prediction that H_2S transforms at 160 GPa to new metallic high-pressure phases with potential superconductivity (maximum estimated T_c = 80 K),[14] which contrasts with a previous supposition that H_2S decomposes into its constituent elements before metallization[63,64] and suggests that new H–S compounds could exist at high pressure. The superconductivities measured by Drozdov *et al.* for samples prepared at low temperature agree well with the estimates for H_2S (Fig. 1a).[14] An accidental finding was that a sample prepared at high temperature exhibited superconductivity at temperatures as high as 203 K under 155 GPa, which originated from the pressure-driven disproportionation of H_2S to H_3S, as confirmed by subsequent theoretical and experimental studies (Fig. 1b).[65–69] Notably, van der Waals compound of $(H_2S)_2H_2$ (*i.e.*, $2H_3S$) was synthesized in 2011 (ref. 70) and H_3S was later predicted to adopt a highly symmetric cubic structure showing a potential of high temperature superconductivity with an estimated $T_c \approx$ 200 K at 200 GPa.[21]

Theoretical studies have demonstrated that strong covalent bonding is a key determinant of the high superconductivity in H_3S, thus providing a new route to design superconducting hydrides. Many attempts have been made to design covalent superconducting hydrides, including H_3Se,[71] PH_2,[72] PH_3,[73,74]

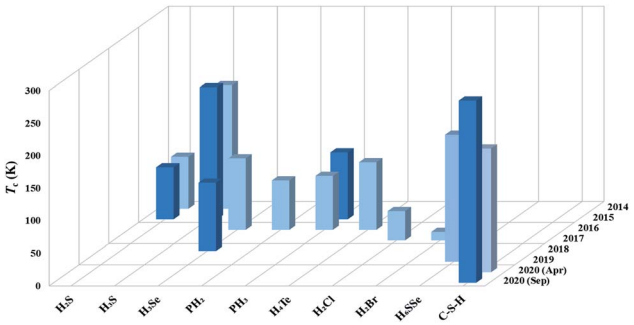

Fig. 2 Computed (light blue) and measured (dark blue) T_c of covalent hydrides since 2014.

TeH_4,[75] $H_2Cl/Br/I$,[76,77] H_6SSe,[78] and C–S–H,[20,41,42] as summarized in Fig. 2. Two independent theoretical studies in early 2020 proposed that the intercalation of methane (CH_4) into the H_3S framework forms a new candidate superconductor, CSH_7, with an estimated T_c of 100–190 K.[41,42] This proposal stimulated subsequent experimental synthesis of CSH_x by compressing elemental C, S, and H_2 above 4 GPa, where a maximum T_c of ~288 K at ~267 GPa (ref. 20) was claimed. However, the undetermined value of x and lack of structural information prevent elucidation of the origin of the superconductivity. We expect future experimental confirmation from an independent group for the record high superconductivity observed in CSH_x and theoretical studies, especially those using CSP, may help provide further details on the structures.

4.1.2 Clathrate hydrides. Another breakthrough was the observation of 260 K superconductivity in the clathrate superhydride LaH_{10} under pressure (Fig. 3a).[22,23] The experimental work investigated two independent theoretical predictions of pressure-stabilized LaH_{10} containing H_{32} cages with high superconductivity (257–288 K at 250 GPa).[6,7] CaH_6 containing sodalite-like H_{24} cages was the first predicted clathrate hydride (in 2012); it shows a high T_c of 235 K at 150 GPa.[79] The same sodalite-like H_{24} cage was later predicted in YH_6 (ref. 40) and MgH_6,[80] which show high T_c values of 264 K and 260 K at 120 GPa. Notably, the predicted high superconductivities of

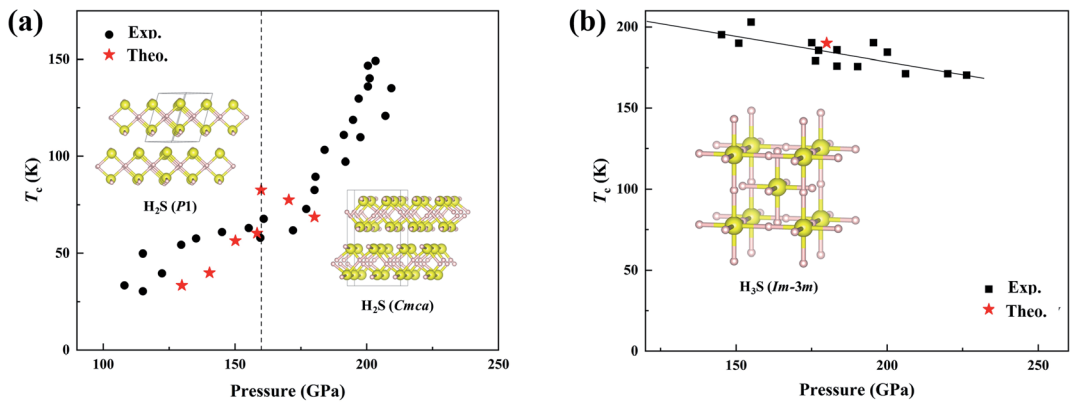

Fig. 1 (a) Comparison of the calculated[14] and measured T_c for H_2S pressurized at low temperature.[15] Insets show two predicted structures.[14] (b) Comparison of the calculated[21] and measured T_c for H_2S pressurized at high temperature.[15] The inset shows the predicted structure.[21]

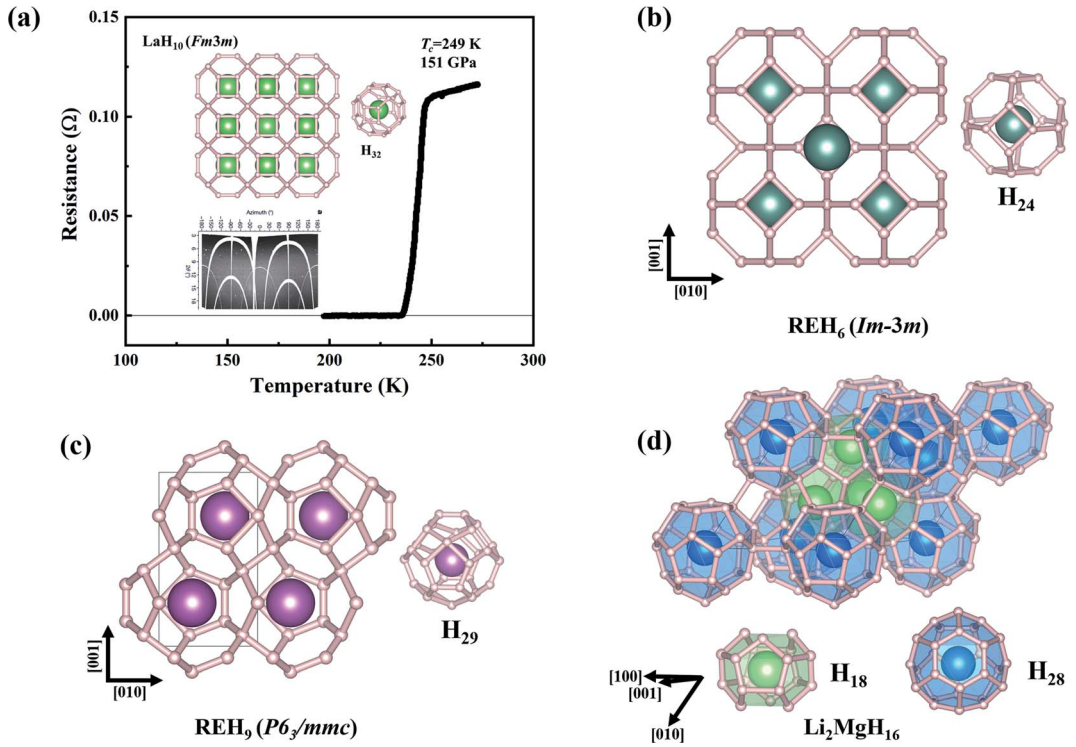

Fig. 3 (a) Measured resistance as a function of temperature of LaH_{10} at 151 GPa.[23] The inset presents the predicted clathrate structure. (b–d) Three typical clathrate structures of superhydrides formed at high pressures.

both CaH_6 and YH_6 have been experimentally confirmed, with T_c values of 215 K (at 172 GPa)[81] and 260 K (at 120 GPa),[82,83] respectively.

Theoretical studies have established the crucial contribution of hydrogen cages to the high superconductivity of the above clathrate hydrides. The cages represent another pathway to the design of high-T_c superconductors, namely, pressure-stabilized clathrate superhydrides. Ref. 11 proposed that there is common rule for the formation of clathrate structures in rare-earth (RE) superhydrides with appearing three different H_{24}, H_{29}, and H_{32} cages in stoichiometric superhydrides of REH_6, REH_9, and REH_{10}, respectively. Subsequent theoretical attempts have further confirmed hydrogen cages as common species at high pressure.[6,7,82–94] Fig. 4a summarizes the cage-structured hydrides predicted at high pressure, most of which show high superconductivity, such as T_c at 473 K in H_{18} + H_{28} cage-structured Li_2MgH_{16},[88] T_c at ~146–243 K in H_{29} cage-structured Y(Ce, Th)H_9,[6,86,94] T_c at 160–303 K in H_{32} cage-structured Y(Th, Ac)H_{10},[6,7,86,93] and T_c at 173 K in H_{40} cage-structured AcH_{12}.[93] Besides the above mentioned experimental confirmation on the theoretical prediction of high superconductivity in CaH_6 and YH_6, subsequent experimental studies have also confirmed high superconductivities in, for example, YH_9,[95] CeH_9,[91] ThH_9,[92] and ThH_{10} (ref. 92) with measured T_c values at ~262, 110, 146 and 160 K, respectively. These successful examples on the theory-orientated finding of high T_c superconductors among pressure-stabilized superhydrides demonstrate that the leading role of theoretical methods.

4.1.3 Challenges and future directions. Theoretical studies have revealed the existence of diverse hydrogen species at high pressure that can lead to high-T_c superconductivity. For example, SrH_6 containing H_3 units, SnH_{12} containing H_4 units, ScH_9 containing H_5 units, and HfH_{10} containing H_{10} units have predicted T_c values of 156 K (250 GPa), 93 K (250 GPa), 163 K (300 GPa), and 234 K (250 GPa), respectively.[96–102] However, currently, no general mechanism can accurately predict the T_c of hydrides. For example, H_{32} cage-structured PrH_{10} has a low T_c of 1.4 K,[89] demonstrating that not all hydrogen cage-structured hydrides possess high superconductivity. Fortunately, there are some indicators of high superconductivity. As summarized in Fig. 4b, high-T_c hydrides will have a high contribution of H-*s* states at the Fermi level; without this, the T_c is low. This represents a convenient way to assess whether a predicted hydride is a high-T_c superconductor, as calculations of the electronic density of states are much less time consuming than those of electron–phonon coupling parameters that are necessary for calculation of T_c.

The superconducting T_c of hydrides can be estimated by using the Allen–Dynes modified McMillan equation, which is suitable for those compounds with electron-phonon coupling parameter (λ) less than 1.5. However, the recent studies have demonstrated that certain superhydrides have very strong electron-phonon coupling parameters λ (*e.g.*, 2.19 for H_3S, 2.69 for CaH_6, and ~4 for Li_2MgH_{16}), posing a challenge to use Allen–Dynes modified McMillan equation for the calculation of the T_c values for the predicted hydrides. An alternative method is to estimate T_c directly from the spectral function ($\alpha^2F(\omega)$) by

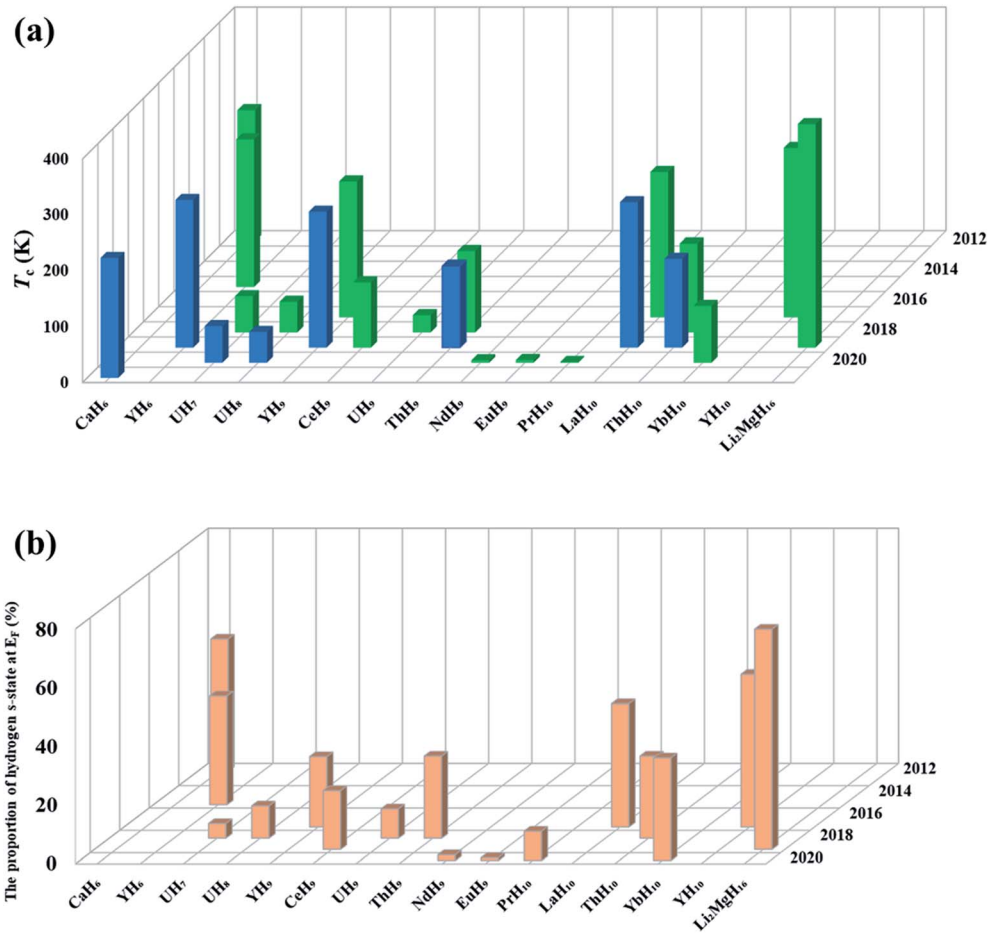

Fig. 4 (a) Summary of the computed (green) and measured (blue) T_c of several typical superconducting superhydrides. (b) Proportion of H-*s* electron states at the Fermi level for selected superconducting superhydrides.

numerically solving the Eliashberg equations,[103] which gives a better description of systems with λ larger than 1.5.

A limitation of high-T_c hydrides is that their stability is maintained only under extremely high pressures, which precludes any immediate practical application. A research aim is therefore to search for superhydrides that can be synthesized at moderate pressures and are quenchable to ambient conditions as metastable phases. Currently, ternary hydrides display high potential as high-T_c superconductors, as exemplified by CSH_x (288 K)[20] and Li_2MgH_{16} (473 K).[88] We expect that the relatively more complex interactions in ternary systems could form hydrides at moderate pressures. Theoretical predictions, especially those employing CSP methods, will undoubtedly play a key role in achieving this goal.

4.2 Polymeric nitrogen

Solid nitrogen at ambient pressure adopts a diatomic molecular form, characterized by strong triple N≡N bonds within each N_2 molecule (Fig. 5a). High pressure can efficiently break the triple bonds to form single N–N bonds, allowing the formation of polymeric phases. The large energy difference between the single (~160 kJ mol^{-1}) and triple (~954 kJ mol^{-1}) bonds means that the transformation from single to triple bonds releases much energy, making polymeric nitrogen or nitrides containing N–N bonds ideal high-energy-density materials. Theoretical studies have guided experimental efforts to synthesize the proposed high-energy-density materials. Here, we provide an overview of recent discoveries initiated by theoretical design of high-energy-density materials at high pressure, specifically polymeric nitrogen crystals and N-rich compounds (Table 2).

4.2.1 Pure nitrogen. This field emerged in 1985, when a new phase of nitrogen solely composed of single-bonded nitrogen atoms was first predicted by computational simulation to be stable at ~50 GPa (ref. 104) (cg-N, Fig. 5b). Experiments have attempted to synthesize cg-N; however, only amorphous products, probably composed of small clusters of nonmolecular phases, were initially obtained during compression at room temperature. In 2004, however, a transparent single-bonded cubic phase was first synthesized at ~110 GPa and 2000 K;[24,25] it was found to be the theoretically predicted cg-N. This successful synthesis, initiated by theoretical design, greatly promoted the exploration of other types of polynitrogen under high pressure. In addition to the three-dimensional cg-N, another polymeric phase of nitrogen with a layered black phosphorus structure (BP–N, Fig. 5c) was also proposed at high

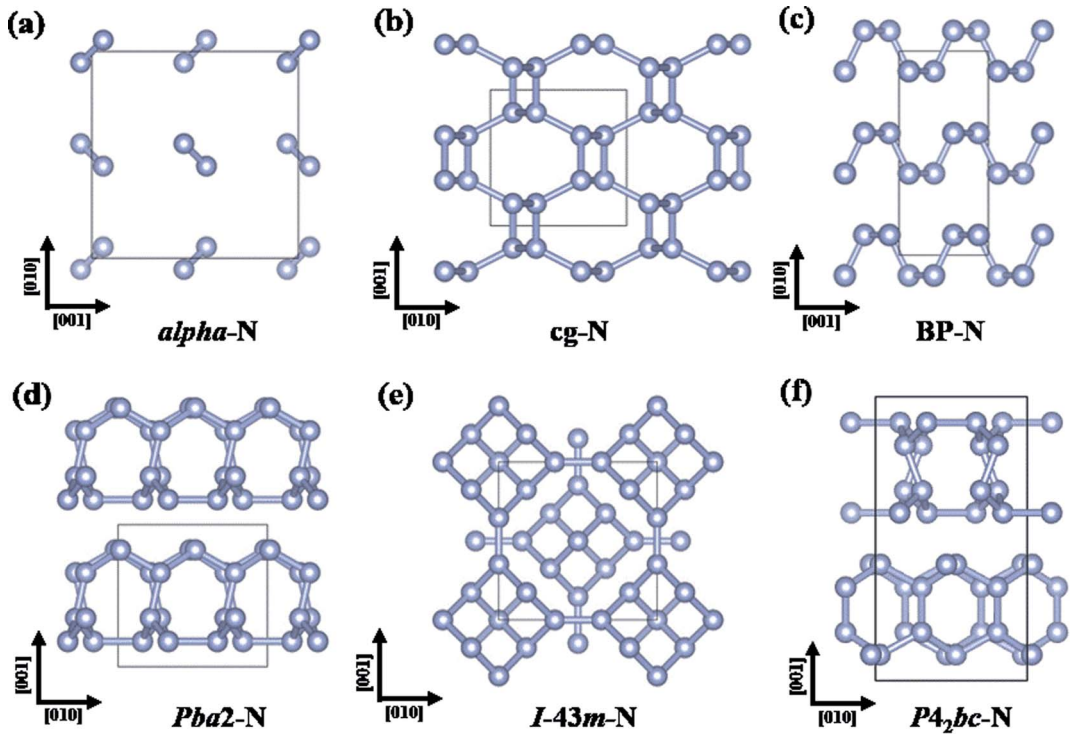

Fig. 5 Crystal structures of (a) *alpha*-N, (b) cg-N, (c) BP-N, (d) *Pba*2-N, (e) *I*-43*m*-N, and (f) $P4_2bc$-N.

pressure.[105] This phase was recently successfully synthesized at 140 GPa, as evidenced by the agreement between the simulated and observed Raman patterns.[106]

Many other stable or metastable polymeric nitrogen phases at high pressures have also been predicted by CSP methods.[26,107–114] Among the most-energetically stable phases, a phase sequence of cg-N → orthorhombic LP-*Pba*2 (188 GPa)[26] → *bcc I*-43*m* (263 GPa)[111] → orthorhombic *Cmca* (2200 GPa)[112] → tetragonal *P*4/*nbm* (2500 GPa)[112] was suggested (Fig. 5b–d). Besides, a tetragonal $P4_2bc$ structure (Fig. 5f) was predicted to have energy indistinguishable from that of the *Pba*2 structure.[111] Among these structures, LP-*Pba*2 and $P4_2bc$ have been experimentally synthesized at 125–180 (ref. 37) and ~250 GPa,[115] respectively.

4.2.2 Nitrogen-rich compounds. Polymeric nitrogen, stabilized by highly compressing pure nitrogen, has yet to be recovered under ambient conditions, precluding its application as a high-energy-density material. Nitrides are potential alternatives that can form single N–N bonds at lower pressure. Alkali metal azides AN_3 (A = Li, Na, K, Rb, or Cs) containing double N=N bonded linear N_3^- anions initially attracted attention, as double N=N bonds with lower bonding energy (418 kJ mol^{-1}) than triple N≡N bonds could transform to single bonds much more easily than pure N_2. Indeed, theoretical studies have shown that azides can polymerize at low pressures of ~50 GPa, with the formation of pseudobenzene N_6 rings containing both double N=N and single N–N bonds (Fig. 6). However, the pressures needed to form three-dimensional polymerized

Table 2 Examples of theory-initiated discovery of polymeric nitrogen under high pressures

Materials	Brief description	Year	References
cg-N	The first theoretical predicted polymetric nitrogen at ~50 GPa	1992	104
	Experimental synthesis of cg-N at 110 GPa and 2000 K	2004	24 and 25
*Pba*2-N	Theoretical prediction of stable layered polymeric N at 188–263 GPa	2009	26
	Experimental synthesis of *Pba*2-N at 125–180 GPa	2014	37
$P4_2bc$-N	Theoretical prediction of a metastable polymeric N	2012	111
	Experimental synthesis of $P4_2bc$-N at 250 GPa	2019	115
LiN_5	Theoretical prediction of stable LiN_5 containing a polymeric N_5 framework above 9.9 GPa	2015	27
	Experimental synthesis of LiN_5 by compressing LiN_3 and N_2 at ~40 GPa	2020	136
	Experimental synthesis of LiN_5 by compressing pure lithium and nitrogen at ~45 GPa	2018	137 and 138
WN_6	Theoretical predictions of stable WN_6 containing N_6 rings at 16 GPa	2017	139
	Theoretical predictions of stable WN_6 containing N_6 rings at 65 GPa	2018	140
	Experimental synthesis of WN_6 at 126 GPa	2021	141

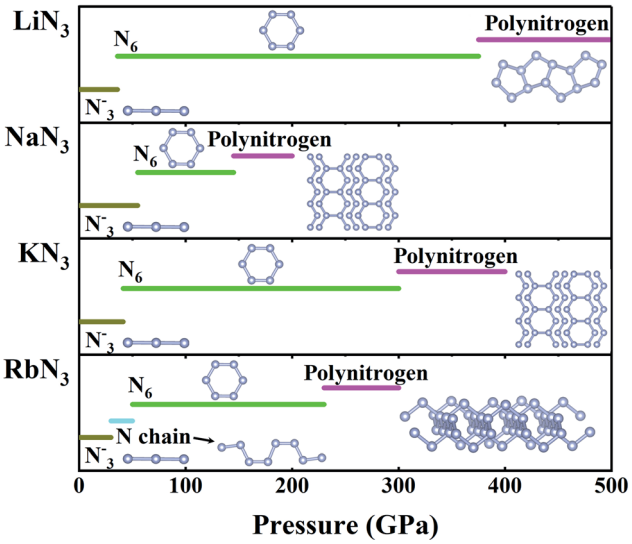

Fig. 6 Polymerization of nitrogen in alkali metal azides at high pressure.

nitrogen networks are unexpectedly high. For example, NaN_3 requires 150 GPa, and other azides require pressures exceeding 200 GPa (Fig. 6).[116–122] Extensive experiments have been performed to investigate the polymerization of nitrogen in azides, and the dissociation of double N=N bonds was only observed in NaN_3 considering the disappearance of molecular vibrations above 120 GPa.[123] However, polymerization of nitrogen has not been observed in other azides, as the experimental pressures considered for other azides are lower than 50 GPa.[124–129] We expect that future high-pressure experiments might observe polymerization of nitrogen in other azides.

Studies have demonstrated that high pressure can stabilize unconventional nitrogen-rich compounds with high ratios of nitrogen, providing another route to polymerization of nitrogen. Theoretical calculations have predicted that many unconventional nitrides, MN_{4-10} (M = Li, Be, Na, Mg, Ca, Cr, Ru, or O_S), stabilize at high pressure.[3,130–135] In 2015, unconventional LiN_5 containing a polymeric N_5^{-1} framework that becomes energetically stable at pressures as low as 9.9 GPa was predicted in addition to conventional LiN_3.[27] The study also proposed compressing solid LiN_3 and N_2 as a feasible way to synthesize LiN_5; subsequent experimental work successfully synthesized LiN_5 by compressing LiN_3 and N_2 at pressures up to ~40 GPa.[136] Two independent experiments also synthesized LiN_5 by compressing pure lithium embedded in a much greater quantity of molecular nitrogen at 45 GPa.[137,138] The discovery of CsN_5 was similar. It was first predicted to be energetically stable at 9.1 GPa, and the first synthesis was achieved by compressing a mixture of CsN_3 and N_2 to 60 GPa.[43] Another example is WN_6, which was hypothesized to contain single-bonded armchair-like N_6 rings and was first proposed to be stable at 16 GPa (ref. 139) or 65 GPa,[140] and it was recently successfully synthesized at a much higher pressure of 126 GPa.[141]

4.2.3 Challenges and future directions. Nitrides indeed belong to a special category, the synthetic pressures of which are sometimes much higher than those predicted, different to the cases in most of other compounds. A plausible explanation is that the triple N≡N bond is the strongest bond in nature, making a need for an extra pressure or temperature to overcome the energy barrier for the transformation of a triple bond into a single bond. For example, in actual experiments, an extra pressure of ~60 GPa evidences as compared to the theoretical one for the synthesis of cg-N and WN_6. However, it is still a challenge to evaluate the exact extra pressure needed to synthesize the predicted nitrides. One might calculate energy barrier by using methods such as climbing image nudged elastic band for a good estimation of the aforementioned extra pressure. Besides the above mentioned theoretical examples that received the subsequent experimental confirmation, many other proposed nitrogen-rich compounds[3,130–135,142–146] are to be verified, representing significant challenges to experimentalists. Furthermore, although nitrogen-rich compounds could be synthesized at low pressure and even recovered under ambient conditions, their energy densities are lower than that (9.7 kJ g^{-1}) of pure cg-N due to the introduction of other elements, for example, 3.48 kJ g^{-1} in MgN_{10} (ref. 147) and 5.39 kJ g^{-1} in BeN_{10}.[147] Theoretical studies have identified two candidate routes to design new materials with high energy density. One is to search for nitrides with extremely high nitrogen contents, such as HeN_{22},[148] whose energy density reaches 10.44 kJ g^{-1}. The other is to design pure polymeric nitrogen by removing the non-N elements from compounds that can be obtained at high pressure; for example, polymeric *t*-N has been predicted to be achievable by removing He from HeN_4 (ref. 149) and to have a high energy density of 11.3 kJ g^{-1}. We expect that further study using CSP methods can help design alternative N-containing high-energy-density materials for their future synthesis.

4.3 Inorganic electrides

Electrides represent a distinct class of ionic compounds, in which electrons distributed in lattice cavities or channels can occupy non-nuclear orbitals and serve as anions individually rather than being attached to atoms. They are potentially useful as catalysts, electron donors, and reducing agents due to their unique physicochemical properties. At the pressures currently achievable, the hybridized valence electrons could be repulsed by core electrons into lattice interstices when compression is sufficiently strong that atomic cores start to overlap, leading to the formation of electrides. Therefore, pressure application is an efficient approach to the design of electrides. Their formation under high pressure is often accompanied by changes in electronic properties, for example, the metal–insulator transition in alkali metals or the emergence of superconductivity.[16,38] Little progress was made in the experimental synthesis of electrides until the development of computational approaches for screening electride materials.[58,150–152] Here, we introduce some important progress in the theory-guided discovery of electrides, including elemental Na and Li and the binary systems of Ca_2N and Sr_5P_3 (Table 3).

4.3.1 Alkali metal electrides. Alkali and alkaline-earth metals such as Li,[38] Na,[16] K,[153] Rb,[153] Cs,[154] Mg,[155] and Ca[156]

Table 3 Examples of theory-initiated discovery of inorganic electrides under high-pressures

Materials	Brief description	Year	References
Na	Na is predicted and observed to form an insulating electride at 200 GPa	2019	16
Li	Li is predicted to form a semiconducting electride at 60–80 GPa	2011	38
	Experimental observation of Li electride above 60 GPa	2011	158 and 159
Ca_2N	Ca_2N is predicted to transform into a zero-dimensional insulating electride at 9.7 GPa	2017	28
	Experimental confirmation of the insulating electride Ca_2N at 11 GPa	2018	161

tend to form electrides at high pressure due to the strong overlap of core electrons from two neighboring atoms.[58] Na is a typical electride whose discovery was guided by theory. In 2019, Ma *et al.* predicted an unusual phenomenon of anti-Wilson transition: a good metal of sodium becomes a transparent insulator at megabar pressures, violating the wisdom of traditional Wilson transition,[16] an accepted trend of high pressures favoring metallicity.[157] Electronic calculations revealed strong localization of valence electrons in the lattice interstices induced by the overlap of core–core electrons, making hP4-Na an electride analogous to the Ni_2In-type structure, where the ionic cores form the Ni sublattice and the interstitial density maxima form the quasiatom In sublattice. Interestingly, photographs taken under combined transmitted and reflected illumination revealed that Na becomes optically transparent at pressures of 200 GPa, signaling a metal-to-insulator transformation. X-ray diffraction (XRD) observation of transparent Na confirmed the hP4 structure of insulating Na, proving the formation of electride Na at high pressure. Li was another alkali metal predicted to form a semiconducting electride phase due to the localization of valence electrons at 60–80 GPa.[38] The electride phase was subsequently observed in two independent experiments.[158,159] Calculations show that the orbital energies of quasiatoms in electrides Li and Na become lower than the valence orbitals of ionic at high pressure, explaining the mechanism to form electride phase.[160]

4.3.2 Binary electrides. Binary compounds, especially those containing excess electrons, have the potential to be electrides. For example, ground-state anti-$CdCl_2$-type Ca_2N was the first observed two-dimensional (2D) electride with excess electrons weakly localized between two positively charged $[Ca_2N]^+$ layers (Fig. 7b). Theoretical work predicted that Ca_2N transforms into a zero-dimensional (0D) electride adopting a tetragonal $I\bar{4}2d$ structure (Fig. 7c) at 9.7 GPa, accompanied by a metal-to-insulator transformation.[28] The predicted structure was subsequently synthesized at 11 GPa, proving the possibility of Ca_2N forming a 0D electride at high pressure.[161] CSP methods have helped in predicting many electrides that can be formed at ambient or high pressures, such as Y_2C,[131] Sr_2N,[52] and Ba_2N[52] at ambient pressure and Na_2He,[5] Li_6P,[162] Na_3S,[163] Ti_2O,[164] Mg_2Xe,[165] and Mg_3O_2 (ref. 166) at high pressures. Among the predicted electride structures, 2D Y_2C,[167] 1D Sr_5P_3,[29] and 0D Na_2He[5] have been experimentally confirmed.

4.3.3 Challenges and future directions. Unconventional compounds stabilized at high pressure may possess excess electrons, making them potential electrides; therefore, high pressure provides many opportunities to search for new electrides. Theoretically, identifying an electride by simulating, for example, the electron localization function, electronic density, or charge-density difference, is easy. However, experimental investigations face significant challenges, as localized electrons are hardly detected. Verification of the theoretically predicted electrides generally involves indirect probes such as XRD, transport, X-ray photoemission spectroscopy, magnetic susceptibility, and angle-resolved photoemission spectroscopy (ARPES) measurements, with comparison of observed and calculated results. An ARPES measurement of Y_2C indicated that electron–hole electride bands exist near the Fermi energy, as predicted by *ab initio* calculations, supporting that Y_2C is indeed a 2D electride. Noteworthy, ARPES only detects ambient-pressure electrides owing to its incompatibility with high-pressure set-ups. Therefore, theoretical simulations play a key role to discover high-pressure electrides.

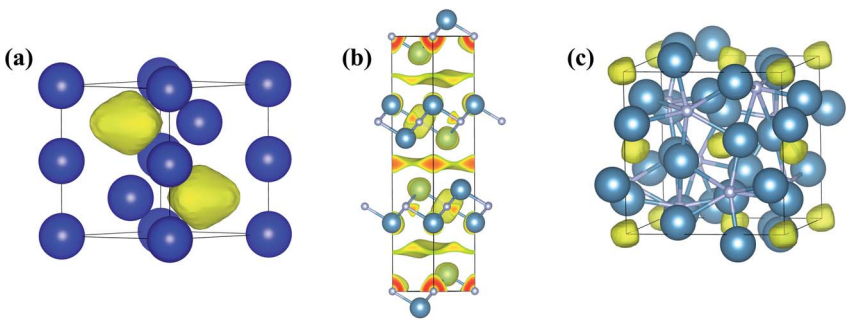

Fig. 7 Three-dimensional electron localization function maps of (a) hP4-Na at 200 GPa, (b) *anti*-$CdCl_2$-type Ca_2N at ambient pressure, and (c) $I42d$ Ca_2N at 20 GPa to show electron localization in the lattice interstices.

Table 4 Examples of theory-initiated discovery of noble gas compounds under high pressures

Materials	Brief description	Year	References
$XeFe_3$ ($XeNi_3$)	Theoretical predictions of stable $XeFe_3$ and $XeNi_3$ above 200 and 150 GPa, respectively	2014	4
	Experimental synthesis of $XeNi_3$ at ~150 GPa	2017	18
	Experimental synthesis of $XeFe_3$ and $XeNi_3$ at 210 and 155 GPa, respectively	2018	19
Xe_3O_2	Theoretical prediction of stable Xe_3O_2 above 75 GPa	2014	30
	Experimental synthesis of Xe_3O_2 at 97 GPa	2016	17
Na_2He	Theoretical prediction and experimental confirmation of Na_2He at high pressure	2017	5

4.4 Chemistry of noble elements

Noble elements are characterized by their full electron shells and chemical inertness. The long-held belief that an element cannot react further if it has full valence orbitals was questioned with the first theoretical proposal of the chemical reaction of Xe by Pauling in 1933 (ref. 168) and disproved with the first synthesis of $XePtF_6$ in 1962 by Neil Bartlett.[169] Noble gases are common in the universe and are generally considered to exist only in planetary atmospheres rather than in their interiors due to their chemical inertness. Recent studies using CSP methods have predicted a large number of noble gas compounds that are stable at high pressures and temperatures corresponding to the conditions inside the earth or large icy planets. These compounds are therefore essential to the understanding of the interior structure of planets.[4,170–177] Here, we summarize the theory-guided synthesis of noble gas compounds, paying particular attention to Xe and He compounds (Table 4).

4.4.1 Xe-bearing compounds. Studies of Earth's atmosphere have shown that more than 90% of the expected amount of Xe is depleted, a finding often referred to as the missing Xe paradox. It represents one of the most challenging enigmas of planetary science. Theoretical studies have provided feasible explanations to help resolve the paradox. Theoretical calculations suggest that Xe could be trapped as solid compounds inside the Earth's inner core, as indicated by the predicted reactions of Xe with Fe and Ni (the main constituents of the core) to form $XeFe_3$ and $XeNi_3$ (ref. 4) (Fig. 8a and b). Subsequently, $XeFe_3$ and $XeNi_3$ have been successfully synthesized at high pressures of 210 and 150 GPa, respectively.[18,19] The XRD patterns of these compounds are well indexed to the predicted structures, highlighting the key role of CSP methods in aiding the discovery of unknown materials.

Theoretical calculations also uncovered the reason for the emergence of chemical activity in Xe at high pressure. The full 5p shell of Xe opens at high pressure, making Xe a 5p-like element with the ability to transfer electrons to Fe or Ni. This form of Xe has been predicted to react with many other elements or molecules at high pressure to produce, for example, Xe_3O_2,[30] XeN_6,[178] LiXe,[179] MgXe,[165] Xe_2F,[180] $Xe_4O_{12}H_{12}$,[181] Xe_2FeO_2,[170] CsXe,[182] and Xe–H_2.[183–185] Among these, Xe_3O_2 and XeN_6 were subsequently synthesized. The reactivity of Xe with O was previously confirmed to occur at pressures as low as 3 GPa, with the formation of the van der Waals compound $Xe(O_2)_2$.[186] Later, CSP methods predicted the formation of a new Xe_3O_2 (Fig. 8c) compound above 75 GPa.[30] Recent experiments successfully synthesized this compound (at 97 GPa) as well as the unpredicted compound Xe_2O_5 (88 GPa).[17] A prediction of Xe–N was made at pressures of 100–300 GPa, with the finding of stable XeN_6 above 146 GPa, indicating the reactivity of Xe with N_2.[178] These elements were later experimentally reacted at much lower pressure (5 GPa) to form the van der Waals compound $Xe(N_2)_2$.[187] Much higher pressures are needed to synthesize the predicted stoichiometric XeN_6.

4.4.2 He-bearing compounds. As the most chemically inert element, helium is generally considered to be uncapturable inside ice giants such as Uranus and Neptune, and it may exist only in their gaseous atmospheres. Surprisingly, recent theoretical and experimental efforts have demonstrated the chemical reactivity of helium at high pressure and temperature conditions *via* a theory-initiated discovery of the He-bearing Na_2He compound (Fig. 8d), which was predicted to be stable above 160 GPa, with later experimental confirmation.[5] The high-pressure chemical activity suggests the possibility of helium being trapped with compounds inside the ice giants. Recent theoretical works have explored possible stable compounds formed by helium and the interior components of ice giants (*e.g.*, CH_4, NH_3, and H_2O). CSP methods have predicted many such compounds at high pressure and temperature conditions corresponding to those in planet interiors, such as $He(NH_3)_2$,[172] $He(H_2O)_2$,[173,174] He_2H_2O,[174] He_2H_2O,[174] He_3CH_4,[176] and $HeCH_4$.[176] Some of these compounds were predicted to have

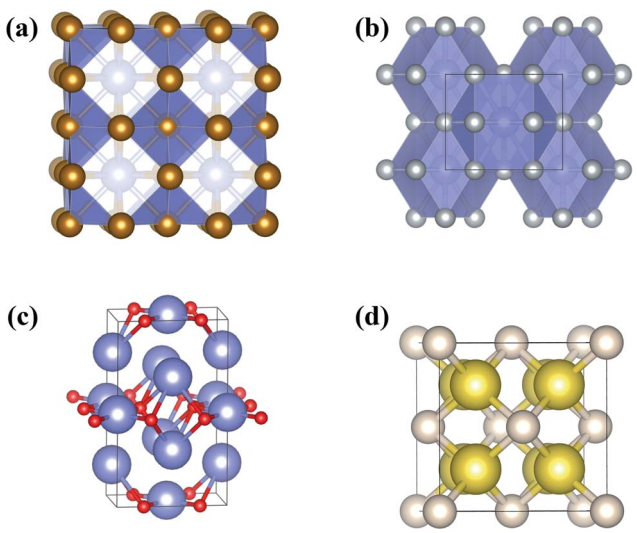

Fig. 8 Predicted and confirmed crystal structures of (a) $XeFe_3$, (b) $XeNi_3$, (c) Xe_3O_2, and (d) Na_2He.

a superionic characteristic. Although these predicted compounds have yet to be confirmed, these theoretical results might be helpful for the understanding of the planet interior models and planets' evolution.

A recent theoretical study demonstrated that helium could also be trapped in Earth's lower mantle by the prediction of stable FeO_2He.[171] Helium was even predicted to react with a broad range of ionic A_2B- and AB_2-type compounds, such as Li_2O, CaF_2, and MgF_2,[188] and react with nitrogen to form stable HeN_4,[149] HeN_6, HeN_{10}, and HeN_{22} (ref. 148) at high pressures. A common feature of these compounds is the formation of host–guest structures with guest helium atoms intercalated into the lattice interstices, with almost no charge transfer between helium and the other elements. These predicted He compounds have yet to be experimentally confirmed.

4.4.3 Challenges and future directions. The formation of stable noble gas compounds at high pressure goes against the traditional notion of nonreactivity in elements with full electron shells. As few of these predicted compounds have been experimentally confirmed, there remain notable challenges for experiments. The confirmed Xe or He compounds reveal two future research directions. One is the continuing exploration of stable compounds formed at high pressures and high temperatures by noble elements with components inside planets (*e.g.*, MgO, FeO_2, SiO_2, Al_2O_3, CaO, $CaSiO_3$, and $MgSiO_3$), with the aim of improving models of planetary interiors. The other is the design of functional materials by stabilizing these compounds at high pressure, as illustrated by the case of high-energy-density *t*-N obtained from pressure-stabilized HeN_4.[149] The incorporation of helium could effectively modulate the structures and properties of known compounds, thus providing a new pathway to design functional materials. Furthermore, other noble elements also show chemical activity at high pressure, with $(N_2)_6Ne_7$ being experimentally observed at above 8 GPa.[189] Therefore, future attention might be paid to pressure-stabilized Ne, Ar, and Ke compounds.

5 Outlook

In addition to the abovementioned examples, other types of functional materials have been frequently discovered at high pressure, such as superhard, ferromagnetic, ferroelectric, optoelectronic, catalytic, negative compressibility, and thermoelectric materials[190] where theory can also play a vital role in aiding the discovery. Though CSP-based theory is quite successful for the design of materials, challenges remain, in particular for large simulation systems, which contain usually a large number of atoms in the simulation cells, reaching several hundreds and thousands of atoms. The number of the candidate structures increases exponentially with the increasing number of atoms in the simulation system, leading to an extremely complex potential energy landscape with a tremendous number of energy minima for a large system.[191] Generally, one has to optimize all candidate structures to find the global energy minima, however, a practical problem is that the much time-consuming geometry optimizations makes it is apparently unaffordable for the available first-principles methods. Also, for ternary or quaternary systems, the existence of huge candidate compositions results in unbearable complicated composition landscape, posing a big challenge for the current first-principle methods to calculate the countlessly possible structures. One strategy might be considered on the development of alternative algorithms that guarantee fast and reliable calculations on total energy and geometry optimization. Force field methods, machine learning potentials,[192] and linear scaling methods (*e.g.*, orbital free density functional theory[193]) might be relied on, but particular caution must be taken for the transferability of the method in dealing with entirely different structures. Besides the use of machine learning potentials, machine learning technique (*e.g.*, deep learning, *etc.*) can offer an alternative opportunity to aid the material discovery. As a data-driven method, machine learning uses large amounts of data to continuously optimize models and to make reasonable predictions under the guidance of algorithms.[194–196] Generally, high-quality data can be selected as training and testing sets from the available material databases, such as Open Quantum Material Database, Material Project, Computational Materials Repository, Inorganic Crystal Structure Database, AFLOWLIB, and CALYPSO structure database, as well as those obtained by local structure optimizations of plenty of structures generated by CSP methods.[197,198]

The products *via* high-pressure experiments are largely influenced by many factors, such as the precursors, the grain size of sample, the rate of pressure rise, as well as the temperature used. The current theoretical methods are ready to predict the static crystal structures at a given pressure and zero temperature, however, the lack of the study on the dynamic process of material formation provides no information about the synthetic pathway. A reaction pathway describes the successive steps at the molecular level that takes place in a chemical reaction, while a deep understanding of all reaction pathways is essential to explore the evolution of a system over time given a set of initial conditions such as precursors, pressure and temperature. This provides insight into the choices of reaction conditions that can affect the overall reaction outcome, purity, and reaction rates.[199,200] The use of CSP simulations in combination with the method for calculations of kinetic energy barriers (KEB) for the chemical reaction or phase transition may help to screen out the possible synthetic routes, thus narrowing down the scope of the experiment trials. To obtain the KEB, one has to find out the minimum energy path and transition state from the astronomically large number of possible solutions. The calculation of KEB can be achieved by a recent reported evolution strategy combining a matrix particle swarm optimization algorithm and an improved nudged elastic band method with the knowledge of the initial state and the final state.[61] However, there is lack of a generally applicable technique on how to account for the dynamic environment of a reacting system with quantum accuracy, posing a challenge for the investigation of the KEB. It is believed that the development of useful strategy to probe the mechanism of chemical reaction is one of the essential issues to accelerate the material discovery initialized by theoretical design.

Data availability

Figures, tables and detailed crystallographic information are available from the corresponding author by request.

Author contributions

All authors contributed to the preparation of the manuscript. M. X. and Y. L. participated in original draft writing and graphic visualization. Y. M. contributed to the substantial revision of the original draft.

Conflicts of interest

There are no conflicts to declare.

Acknowledgements

This work was supported by the National Natural Science Foundation of China (Grant No. 12074154, 11904142, and 11722433), the Major Program of the National Natural Science Foundation of China (Grant No. 52090024), and the National Key R&D Program of China (Grant No. 2018YFA0305900).

References

1 L. Zhang, Y. Wang, J. Lv and Y. Ma, *Nat. Rev. Mater.*, 2017, **2**, 17005.
2 M. Miao, Y. Sun, E. Zurek and H. Lin, *Nat. Rev. Chem.*, 2020, **4**, 508–527.
3 Y. Li, J. Hao, H. Liu, S. Lu and J. S. Tse, *Phys. Rev. Lett.*, 2015, **115**, 105502.
4 L. Zhu, H. Liu, C. J. Pickard, G. Zou and Y. Ma, *Nat. Chem.*, 2014, **6**, 644–648.
5 X. Dong, A. R. Oganov, A. F. Goncharov, E. Stavrou, S. Lobanov, G. Saleh, G.-R. Qian, Q. Zhu, C. Gatti, V. L. Deringer, R. Dronskowski, X.-F. Zhou, V. B. Prakapenka, Z. Konôpková, I. A. Popov, A. I. Boldyrev and H.-T. Wang, *Nat. Chem.*, 2017, **9**, 440–445.
6 H. Liu, I. I. Naumov, R. Hoffmann, N. W. Ashcroft and R. J. Hemley, *Proc. Natl. Acad. Sci. U. S. A.*, 2017, **114**, 6990–6995.
7 F. Peng, Y. Sun, C. J. Pickard, R. J. Needs, Q. Wu and Y. Ma, *Phys. Rev. Lett.*, 2017, **119**, 107001.
8 W. Zhang, A. R. Oganov, A. F. Goncharov, Q. Zhu, S. E. Boulfelfel, A. O. Lyakhov, E. Stavrou, M. Somayazulu, V. B. Prakapenka and Z. Konopkova, *Science*, 2013, **342**, 1502–1505.
9 R. J. Hemley, *High Press. Res.*, 2010, **30**, 581–619.
10 Z. Jenei, E. F. O'Bannon, S. T. Weir, H. Cynn, M. J. Lipp and W. J. Evans, *Nat. Commun.*, 2018, **9**, 3563.
11 L. Dubrovinsky, N. Dubrovinskaia, E. Bykova, M. Bykov, V. Prakapenka, C. Prescher, K. Glazyrin, H. P. Liermann, M. Hanfland, M. Ekholm, Q. Feng, L. V. Pourovskii, M. I. Katsnelson, J. M. Wills and I. A. Abrikosov, *Nature*, 2015, **525**, 226–229.
12 N. Dubrovinskaia, L. Dubrovinsky, N. A. Solopova, A. Abakumov, S. Turner, M. Hanfland, E. Bykova, M. Bykov, C. Prescher, V. B. Prakapenka, S. Petitgirard, I. Chuvashova, B. Gasharova, Y. Mathis, P. Ershov, I. Snigireva and A. Snigirev, *Sci. Adv.*, 2016, **2**, 1–12.
13 W. A. Phelan, J. Zahn, Z. Kennedy and T. M. McQueen, *J. Solid State Chem.*, 2019, **270**, 705–709.
14 Y. Li, J. Hao, H. Liu, Y. Li and Y. Ma, *J. Chem. Phys.*, 2014, **140**, 174712.
15 A. P. Drozdov, M. I. Eremets, I. A. Troyan, V. Ksenofontov and S. I. Shylin, *Nature*, 2015, **525**, 73–76.
16 Y. Ma, M. Eremets, A. R. Oganov, Y. Xie, I. Trojan, S. Medvedev, A. O. Lyakhov, M. Valle and V. Prakapenka, *Nature*, 2009, **458**, 182–185.
17 A. Dewaele, N. Worth, C. J. Pickard, R. J. Needs, S. Pascarelli, O. Mathon, M. Mezouar and T. Irifune, *Nat. Chem.*, 2016, **8**, 784–790.
18 A. Dewaele, C. M. Pépin, G. Geneste and G. Garbarino, *High Press. Res.*, 2017, **37**, 137–146.
19 E. Stavrou, Y. Yao, A. F. Goncharov, S. S. Lobanov, J. M. Zaug, H. Liu, E. Greenberg and V. B. Prakapenka, *Phys. Rev. Lett.*, 2018, **120**, 096001.
20 E. Snider, N. Dasenbrock-Gammon, R. McBride, M. Debessai, H. Vindana, K. Vencatasamy, K. V. Lawler, A. Salamat and R. P. Dias, *Nature*, 2020, **586**, 373–377.
21 D. Duan, Y. Liu, F. Tian, D. Li, X. Huang, Z. Zhao, H. Yu, B. Liu, W. Tian and T. Cui, *Sci. Rep.*, 2015, **4**, 6968.
22 M. Somayazulu, M. Ahart, A. K. Mishra, Z. M. Geballe, M. Baldini, Y. Meng, V. V. Struzhkin and R. J. Hemley, *Phys. Rev. Lett.*, 2019, **122**, 027001.
23 A. P. Drozdov, P. P. Kong, V. S. Minkov, S. P. Besedin, M. A. Kuzovnikov, S. Mozaffari, L. Balicas, F. F. Balakirev, D. E. Graf, V. B. Prakapenka, E. Greenberg, D. A. Knyazev, M. Tkacz and M. I. Eremets, *Nature*, 2019, **569**, 528–531.
24 M. I. Eremets, A. G. Gavriliuk, I. A. Trojan, D. A. Dzivenko and R. Boehler, *Nat. Mater.*, 2004, **3**, 558–563.
25 E. Gregoryanz, A. F. Goncharov, C. Sanloup, M. Somayazulu, H. Mao and R. J. Hemley, *J. Chem. Phys.*, 2007, **126**, 184505.
26 Y. Ma, A. R. Oganov, Z. Li, Y. Xie and J. Kotakoski, *Phys. Rev. Lett.*, 2009, **102**, 065501.
27 F. Peng, Y. Yao, H. Liu and Y. Ma, *J. Phys. Chem. Lett.*, 2015, **6**, 2363–2366.
28 Y. Zhang, W. Wu, Y. Wang, S. A. Yang and Y. Ma, *J. Am. Chem. Soc.*, 2017, **139**, 13798–13803.
29 J. Wang, K. Hanzawa, H. Hiramatsu, J. Kim, N. Umezawa, K. Iwanaka, T. Tada and H. Hosono, *J. Am. Chem. Soc.*, 2017, **139**, 15668–15680.
30 A. Hermann and P. Schwerdtfeger, *J. Phys. Chem. Lett.*, 2014, **5**, 4336–4342.
31 E. Zurek and T. Bi, *J. Chem. Phys.*, 2019, **150**, 050901.
32 C. J. Pickard, I. Errea and M. I. Eremets, *Annu. Rev. Condens. Matter Phys.*, 2020, **11**, 57–76.
33 J. A. Flores-Livas, L. Boeri, A. Sanna, G. Profeta, R. Arita and M. Eremets, *Phys. Rep.*, 2020, **856**, 1–78.
34 F. P. Bundy, *J. Chem. Phys.*, 1963, **38**, 631–643.

35 Y. Li, Y. Wang, C. J. Pickard, R. J. Needs, Y. Wang and Y. Ma, *Phys. Rev. Lett.*, 2015, **114**, 125501.
36 W. Feng, S. Cui and M. Feng, *J. Phys. Chem. Solids*, 2014, **75**, 803–807.
37 D. Tomasino, M. Kim, J. Smith and C.-S. Yoo, *Phys. Rev. Lett.*, 2014, **113**, 205502.
38 J. Lv, Y. Wang, L. Zhu and Y. Ma, *Phys. Rev. Lett.*, 2011, **106**, 015503.
39 M. Miao, *Nat. Chem.*, 2013, **5**, 846–852.
40 Y. Li, J. Hao, H. Liu, J. S. Tse, Y. Wang and Y. Ma, *Sci. Rep.*, 2015, **5**, 9948.
41 Y. Sun, Y. Tian, B. Jiang, X. Li, H. Li, T. Iitaka, X. Zhong and Y. Xie, *Phys. Rev. B*, 2020, **101**, 174102.
42 W. Cui, T. Bi, J. Shi, Y. Li, H. Liu, E. Zurek and R. J. Hemley, *Phys. Rev. B*, 2020, **101**, 134504.
43 B. A. Steele, E. Stavrou, J. C. Crowhurst, J. M. Zaug, V. B. Prakapenka and I. I. Oleynik, *Chem. Mater.*, 2017, **29**, 735–741.
44 Y. Wang, J. Lv, L. Zhu and Y. Ma, *Phys. Rev. B: Condens. Matter Mater. Phys.*, 2010, **82**, 094116.
45 Y. Wang, J. Lv, L. Zhu and Y. Ma, *Comput. Phys. Commun.*, 2012, **183**, 2063–2070.
46 C. J. Pickard and R. J. Needs, *J. Phys. Condens. Matter*, 2011, **23**, 053201.
47 C. W. Glass, A. R. Oganov and N. Hansen, *Comput. Phys. Commun.*, 2006, **175**, 713–720.
48 D. C. Lonie and E. Zurek, *Comput. Phys. Commun.*, 2011, **182**, 372–387.
49 G. Trimarchi and A. Zunger, *Phys. Rev. B: Condens. Matter Mater. Phys.*, 2007, **75**, 104113.
50 S. Bahmann and J. Kortus, *Comput. Phys. Commun.*, 2013, **184**, 1618–1625.
51 J. Lv, Y. Wang, L. Zhu and Y. Ma, *J. Chem. Phys.*, 2012, **137**, 084104.
52 Y. Wang, M. Miao, J. Lv, L. Zhu, K. Yin, H. Liu and Y. Ma, *J. Chem. Phys.*, 2012, **137**, 224108.
53 M. Xu, C. Huang, Y. Li, S. Liu, X. Zhong, P. Jena, E. Kan and Y. Wang, *Phys. Rev. Lett.*, 2020, **124**, 067602.
54 X. Zhang, Y. Wang, J. Lv, C. Zhu, Q. Li, M. Zhang, Q. Li and Y. Ma, *J. Chem. Phys.*, 2013, **138**, 114101.
55 S. Lu, Y. Wang, H. Liu, M. Miao and Y. Ma, *Nat. Commun.*, 2014, **5**, 3666.
56 B. Gao, X. Shao, J. Lv, Y. Wang and Y. Ma, *J. Phys. Chem. C*, 2015, **119**, 20111–20118.
57 P. Gao, Q. Tong, J. Lv, Y. Wang and Y. Ma, *Comput. Phys. Commun.*, 2017, **213**, 40–45.
58 Y. Zhang, H. Wang, Y. Wang, L. Zhang and Y. Ma, *Phys. Rev. X*, 2017, **7**, 011017.
59 P. Gao, S. Wang, J. Lv, Y. Wang and Y. Ma, *RSC Adv.*, 2017, **7**, 39869–39876.
60 B. Gao, P. Gao, S. Lu, J. Lv, Y. Wang and Y. Ma, *Sci. Bull.*, 2019, **64**, 301–309.
61 K. Yin, P. Gao, X. Shao, B. Gao, H. Liu, J. Lv, J. S. Tse, Y. Wang and Y. Ma, *npj Comput. Mater.*, 2020, **6**, 16.
62 N. W. Ashcroft, *Phys. Rev. Lett.*, 2004, **92**, 187002.
63 M. Sakashita, H. Yamawaki, H. Fujihisa, K. Aoki, S. Sasaki and H. Shimizu, *Phys. Rev. Lett.*, 1997, **79**, 1082–1085.
64 R. Rousseau, M. Boero, M. Bernasconi, M. Parrinello and K. Terakura, *Phys. Rev. Lett.*, 2000, **85**, 1254–1257.
65 N. Bernstein, C. S. Hellberg, M. D. Johannes, I. I. Mazin and M. J. Mehl, *Phys. Rev. B: Condens. Matter Mater. Phys.*, 2015, **91**, 060511.
66 Y. Li, L. Wang, H. Liu, Y. Zhang, J. Hao, C. J. Pickard, J. R. Nelson, R. J. Needs, W. Li, Y. Huang, I. Errea, M. Calandra, F. Mauri and Y. Ma, *Phys. Rev. B*, 2016, **93**, 020103.
67 I. Errea, M. Calandra, C. J. Pickard, J. Nelson, R. J. Needs, Y. Li, H. Liu, Y. Zhang, Y. Ma and F. Mauri, *Phys. Rev. Lett.*, 2015, **114**, 157004.
68 D. Duan, X. Huang, F. Tian, D. Li, H. Yu, Y. Liu, Y. Ma, B. Liu and T. Cui, *Phys. Rev. B: Condens. Matter Mater. Phys.*, 2015, **91**, 180502.
69 M. Einaga, M. Sakata, T. Ishikawa, K. Shimizu, M. I. Eremets, A. P. Drozdov, I. A. Troyan, N. Hirao and Y. Ohishi, *Nat. Phys.*, 2016, **12**, 835–838.
70 T. A. Strobel, P. Ganesh, M. Somayazulu, P. R. C. Kent and R. J. Hemley, *Phys. Rev. Lett.*, 2011, **107**, 255503.
71 S. Zhang, Y. Wang, J. Zhang, H. Liu, X. Zhong, H.-F. Song, G. Yang, L. Zhang and Y. Ma, *Sci. Rep.*, 2015, **5**, 15433.
72 A. Shamp, T. Terpstra, T. Bi, Z. Falls, P. Avery and E. Zurek, *J. Am. Chem. Soc.*, 2016, **138**, 1884–1892.
73 Y. Yuan, Y. Li, G. Fang, G. Liu, C. Pei, X. Li, H. Zheng, K. Yang and L. Wang, *Natl. Sci. Rev.*, 2019, **6**, 524–531.
74 H. Liu, Y. Li, G. Gao, J. S. Tse and I. I. Naumov, *J. Phys. Chem. C*, 2016, **120**, 3458–3461.
75 X. Zhong, H. Wang, J. Zhang, H. Liu, S. Zhang, H.-F. Song, G. Yang, L. Zhang and Y. Ma, *Phys. Rev. Lett.*, 2016, **116**, 057002.
76 D. Duan, F. Tian, Y. Liu, X. Huang, D. Li, H. Yu, Y. Ma, B. Liu and T. Cui, *Phys. Chem. Chem. Phys.*, 2015, **17**, 32335–32340.
77 Q. Zeng, S. Yu, D. Li, A. R. Oganov and G. Frapper, *Phys. Chem. Chem. Phys.*, 2017, **19**, 8236–8242.
78 B. Liu, W. Cui, J. Shi, L. Zhu, J. Chen, S. Lin, R. Su, J. Ma, K. Yang, M. Xu, J. Hao, A. P. Durajski, J. Qi, Y. Li and Y. Li, *Phys. Rev. B*, 2018, **98**, 174101.
79 H. Wang, J. S. Tse, K. Tanaka, T. Iitaka and Y. Ma, *Proc. Natl. Acad. Sci. U. S. A.*, 2012, **109**, 6463–6466.
80 X. Feng, J. Zhang, G. Gao, H. Liu and H. Wang, *RSC Adv.*, 2015, **5**, 59292–59296.
81 L. Ma, K. Wang, Y. Xie, X. Yang, Y. Wang, M. Zhou, H. Liu, G. Liu, H. Wang and Y. Ma, 2021, arXiv:2103.16282v1.
82 I. A. Troyan, D. V. Semenok, A. G. Kvashnin, A. V. Sadakov, O. A. Sobolevskiy, V. M. Pudalov, A. G. Ivanova, V. B. Prakapenka, E. Greenberg, A. G. Gavriliuk, I. S. Lyubutin, V. V. Struzhkin, A. Bergara, I. Errea, R. Bianco, M. Calandra, F. Mauri, L. Monacelli, R. Akashi and A. R. Oganov, *Adv. Mater.*, 2021, 2006832.
83 P. P. Kong, V. S. Minkov, M. A. Kuzovnikov, A. P. Drozdov, S. P. Besedin, S. Mozaffari, L. Balicas, F. F. Balakirev, V. B. Prakapenka, S. Chariton, D. A. Knyazev, E. Greenberg and M. I. Eremets, *Nat. Commun.*, 2021, **12**, 1–9.

84 D. Zhou, D. V. Semenok, H. Xie, X. Huang, D. Duan, A. Aperis, P. M. Oppeneer, M. Galasso, A. I. Kartsev, A. G. Kvashnin, A. R. Oganov and T. Cui, *J. Am. Chem. Soc.*, 2020, **142**, 2803–2811.
85 L. Ma, M. Zhou, Y. Wang, S. Kawaguchi, Y. Ohishi, F. Peng, H. Liu, G. Liu, H. Wang and Y. Ma, *Phys. Rev. Res.*, 2021, **3**, 043107.
86 A. G. Kvashnin, D. V. Semenok, I. A. Kruglov, I. A. Wrona and A. R. Oganov, *ACS Appl. Mater. Interfaces*, 2018, **10**, 43809–43816.
87 Y. Li, J. Hao, H. Liu, J. S. Tse, Y. Wang and Y. Ma, *Sci. Rep.*, 2015, **5**, 9948.
88 Y. Sun, J. Lv, Y. Xie, H. Liu and Y. Ma, *Phys. Rev. Lett.*, 2019, **123**, 097001.
89 W. Sun, X. Kuang, H. D. J. Keen, C. Lu and A. Hermann, *Phys. Rev. B*, 2020, **102**, 144524.
90 M. Peña-Alvarez, J. Binns, A. Hermann, L. C. Kelsall, P. Dalladay-Simpson, E. Gregoryanz and R. T. Howie, *Phys. Rev. B*, 2019, **100**, 184109.
91 N. P. Salke, M. M. Davari Esfahani, Y. Zhang, I. A. Kruglov, J. Zhou, Y. Wang, E. Greenberg, V. B. Prakapenka, J. Liu, A. R. Oganov and J.-F. Lin, *Nat. Commun.*, 2019, **10**, 4453.
92 D. V. Semenok, A. G. Kvashnin, A. G. Ivanova, V. Svitlyk, V. Y. Fominski, A. V. Sadakov, O. A. Sobolevskiy, V. M. Pudalov, I. A. Troyan and A. R. Oganov, *Mater. Today*, 2020, **33**, 36–44.
93 D. V. Semenok, A. G. Kvashnin, I. A. Kruglov and A. R. Oganov, *J. Phys. Chem. Lett.*, 2018, **9**, 1920–1926.
94 X. Li, X. Huang, D. Duan, C. J. Pickard, D. Zhou, H. Xie, Q. Zhuang, Y. Huang, Q. Zhou, B. Liu and T. Cui, *Nat. Commun.*, 2019, **10**, 3461.
95 E. Snider, N. Dasenbrock-Gammon, R. McBride, X. Wang, N. Meyers, K. V Lawler, E. Zurek, A. Salamat and R. P. Dias, *Phys. Rev. Lett.*, 2021, **126**, 117003.
96 H. Xie, Y. Yao, X. Feng, D. Duan, H. Song, Z. Zhang, S. Jiang, S. A. T. Redfern, V. Z. Kresin, C. J. Pickard and T. Cui, *Phys. Rev. Lett.*, 2020, **125**, 217001.
97 D. Zhou, X. Jin, X. Meng, G. Bao, Y. Ma, B. Liu and T. Cui, *Phys. Rev. B: Condens. Matter Mater. Phys.*, 2012, **86**, 014118.
98 J. Hooper, B. Altintas, A. Shamp and E. Zurek, *J. Phys. Chem. C*, 2013, **117**, 2982–2992.
99 Y. Liu, D. Duan, F. Tian, H. Liu, C. Wang, X. Huang, D. Li, Y. Ma, B. Liu and T. Cui, *Inorg. Chem.*, 2015, **54**, 9924–9928.
100 Z. Wang, H. Wang, J. S. Tse, T. Iitaka and Y. Ma, *Chem. Sci.*, 2015, **6**, 522–526.
101 Y. Wang, H. Wang, J. S. Tse, T. Iitaka and Y. Ma, *Phys. Chem. Chem. Phys.*, 2015, **17**, 19379–19385.
102 X. Ye, N. Zarifi, E. Zurek, R. Hoffmann and N. W. Ashcroft, *J. Phys. Chem. C*, 2018, **122**, 6298–6309.
103 G. M. Eliashberg, *Sov. Phys. JETP*, 1960, **11**, 696.
104 A. K. McMahan and R. LeSar, *Phys. Rev. Lett.*, 1985, **54**, 1929–1932.
105 C. Mailhiot, L. H. Yang and A. K. McMahan, *Phys. Rev. B: Condens. Matter Mater. Phys.*, 1992, **46**, 14419–14435.
106 D. Laniel, B. Winkler, T. Fedotenko, A. Pakhomova, S. Chariton, V. Milman, V. Prakapenka, L. Dubrovinsky and N. Dubrovinskaia, *Phys. Rev. Lett.*, 2020, **124**, 216001.
107 M. M. G. Alemany and J. L. Martins, *Phys. Rev. B: Condens. Matter Mater. Phys.*, 2003, **68**, 024110.
108 W. D. Mattson, D. Sanchez-Portal, S. Chiesa and R. M. Martin, *Phys. Rev. Lett.*, 2004, **93**, 125501.
109 F. Zahariev, A. Hu, J. Hooper, F. Zhang and T. Woo, *Phys. Rev. B: Condens. Matter Mater. Phys.*, 2005, **72**, 214108.
110 C. J. Pickard and R. J. Needs, *Phys. Rev. Lett.*, 2009, **102**, 125702.
111 X. Wang, Y. Wang, M. Miao, X. Zhong, J. Lv, T. Cui, J. Li, L. Chen, C. J. Pickard and Y. Ma, *Phys. Rev. Lett.*, 2012, **109**, 175502.
112 J. Sun, M. Martinez-Canales, D. D. Klug, C. J. Pickard and R. J. Needs, *Phys. Rev. Lett.*, 2013, **111**, 175502.
113 M. J. Greschner, M. Zhang, A. Majumdar, H. Liu, F. Peng, J. S. Tse and Y. Yao, *J. Phys. Chem. A*, 2016, **120**, 2920–2925.
114 S. Liu, L. Zhao, M. Yao, M. Miao and B. Liu, *Adv. Sci.*, 2020, **7**, 1902320.
115 D. Laniel, G. Geneste, G. Weck, M. Mezouar and P. Loubeyre, *Phys. Rev. Lett.*, 2019, **122**, 066001.
116 J. Zhang, Z. Zeng, H.-Q. Lin and Y.-L. Li, *Sci. Rep.*, 2015, **4**, 4358.
117 X. Wang, J. Li, N. Xu, H. Zhu, Z. Hu and L. Chen, *Sci. Rep.*, 2015, **5**, 16677.
118 J. Li, X. Wang, N. Xu, D. Li, D. Wang and L. Chen, *Europhys. Lett.*, 2013, **104**, 16005.
119 X. Wang, J. Li, J. Botana, M. Zhang, H. Zhu, L. Chen, H. Liu, T. Cui and M. Miao, *J. Chem. Phys.*, 2013, **139**, 164710.
120 M. Zhang, H. Yan, Q. Wei, H. Wang and Z. Wu, *Europhys. Lett.*, 2013, **101**, 26004.
121 X. Huang, D. Li, F. Li, X. Jin, S. Jiang, W. Li, X. Yang, Q. Zhou, B. Zou, Q. Cui, B. Liu and T. Cui, *J. Phys. Chem. C*, 2012, **116**, 9744–9749.
122 S. A. Medvedev, I. A. Trojan, M. I. Eremets, T. Palasyuk, T. M. Klapötke and J. Evers, *J. Phys. Condens. Matter*, 2009, **21**, 195404.
123 M. I. Eremets, M. Y. Popov, I. A. Trojan, V. N. Denisov, R. Boehler and R. J. Hemley, *J. Chem. Phys.*, 2004, **120**, 10618–10623.
124 C. Ji, F. Zhang, D. Hou, H. Zhu, J. Wu, M.-C. Chyu, V. I. Levitas and Y. Ma, *J. Phys. Chem. Solids*, 2011, **72**, 736–739.
125 D. Hou, F. Zhang, C. Ji, T. Hannon, H. Zhu, J. Wu and Y. Ma, *Phys. Rev. B: Condens. Matter Mater. Phys.*, 2011, **84**, 064127.
126 C. Ji, R. Zheng, D. Hou, H. Zhu, J. Wu, M.-C. Chyu and Y. Ma, *J. Appl. Phys.*, 2012, **111**, 112613.
127 D. Li, X. Wu, J. Jiang, X. Wang, J. Zhang, Q. Cui and H. Zhu, *Appl. Phys. Lett.*, 2014, **105**, 071903.
128 D. Li, F. Li, Y. Li, X. Wu, G. Fu, Z. Liu, X. Wang, Q. Cui and H. Zhu, *J. Phys. Chem. C*, 2015, **119**, 16870–16878.
129 H. Zhu, F. Zhang, C. Ji, D. Hou, J. Wu, T. Hannon and Y. Ma, *J. Appl. Phys.*, 2013, **113**, 033511.
130 Z. Zhao, K. Bao, D. Li, D. Duan, F. Tian, X. Jin, C. Chen, X. Huang, B. Liu and T. Cui, *Sci. Rep.*, 2015, **4**, 4797.
131 S. Zhu, F. Peng, H. Liu, A. Majumdar, T. Gao and Y. Yao, *Inorg. Chem.*, 2016, **55**, 7550–7555.

132 Y. Zhang, L. Wu, B. Wan, Y. Lin, Q. Hu, Y. Zhao, R. Gao, Z. Li, J. Zhang and H. Gou, *Sci. Rep.*, 2016, **6**, 33506.
133 S. Zhang, Z. Zhao, L. Liu and G. Yang, *J. Power Sources*, 2017, **365**, 155–161.
134 S. Yu, B. Huang, Q. Zeng, A. R. Oganov, L. Zhang and G. Frapper, *J. Phys. Chem. C*, 2017, **121**, 11037–11046.
135 B. A. Steele and I. I. Oleynik, *J. Phys. Chem. A*, 2017, **121**, 8955–8961.
136 M. Zhou, M. Sui, X. Shi, Z. Zhao, L. Guo, B. Liu, R. Liu, P. Wang and B. Liu, *J. Phys. Chem. C*, 2020, **124**, 11825–11830.
137 D. Laniel, G. Weck, G. Gaiffe, G. Garbarino and P. Loubeyre, *J. Phys. Chem. Lett.*, 2018, **9**, 1600–1604.
138 D. Laniel, G. Weck and P. Loubeyre, *Inorg. Chem.*, 2018, **57**, 10685–10693.
139 Q. Li, L. Sha, C. Zhu and Y. Yao, *Europhys. Lett.*, 2017, **118**, 46001.
140 K. Xia, H. Gao, C. Liu, J. Yuan, J. Sun, H.-T. Wang and D. Xing, *Sci. Bull.*, 2018, **63**, 817–824.
141 N. P. Salke, K. Xia, S. Fu, Y. Zhang, E. Greenberg, V. B. Prakapenka, J. Liu, J. Sun and J.-F. Lin, *Phys. Rev. Lett.*, 2021, **126**, 065702.
142 F. Peng, Y. Ma, A. Hermann and M. Miao, *Phys. Rev. Mater.*, 2020, **4**, 103610.
143 Z. Raza, C. J. Pickard, C. Pinilla and A. M. Saitta, *Phys. Rev. Lett.*, 2013, **111**, 235501.
144 Z. Liu, D. Li, S. Wei, Y. Liu, F. Tian, D. Duan and T. Cui, *Phys. Lett. A*, 2019, **383**, 125859.
145 K. Yin, Y. Wang, H. Liu, F. Peng and L. Zhang, *J. Mater. Chem. A*, 2015, **3**, 4188–4194.
146 W. Wang, H. Wang, Y. Liu, D. Li, F. Tian, D. Duan, H. Yu and T. Cui, *Inorg. Chem.*, 2019, **58**, 2397–2402.
147 K. Xia, X. Zheng, J. Yuan, C. Liu, H. Gao, Q. Wu and J. Sun, *J. Phys. Chem. C*, 2019, **123**, 10205–10211.
148 J. Hou, X.-J. Weng, A. R. Oganov, X. Shao, G. Gao, X. Dong, H.-T. Wang, Y. Tian and X.-F. Zhou, *Phys. Rev. B*, 2021, **103**, L060102.
149 Y. Li, X. Feng, H. Liu, J. Hao, S. A. T. Redfern, W. Lei, D. Liu and Y. Ma, *Nat. Commun.*, 2018, **9**, 722.
150 A. R. Oganov, C. J. Pickard, Q. Zhu and R. J. Needs, *Nat. Rev. Mater.*, 2019, **4**, 331–348.
151 A. R. Oganov, *Modern Methods of Crystal Structure Prediction*, Wiley-VCH Verlag GmbH & Co. KGaA, Weinheim, Germany, 2010.
152 T. Inoshita, S. Jeong, N. Hamada and H. Hosono, *Phys. Rev. X*, 2014, **4**, 031023.
153 Y. Ma, A. R. Oganov and Y. Xie, *Phys. Rev. B: Condens. Matter Mater. Phys.*, 2008, **78**, 014102.
154 K. Takemura, N. E. Christensen, D. L. Novikov, K. Syassen, U. Schwarz and M. Hanfland, *Phys. Rev. B: Condens. Matter Mater. Phys.*, 2000, **61**, 14399–14404.
155 P. Li, G. Gao, Y. Wang and Y. Ma, *J. Phys. Chem. C*, 2010, **114**, 21745–21749.
156 H. L. Skriver, *Phys. Rev. Lett.*, 1982, **49**, 1768–1772.
157 A. H. Wilson, *Proc. R. Soc. Lond. - Ser. A Contain. Pap. a Math. Phys. Character*, 1932, **138**, 594–606.
158 C. L. Guillaume, E. Gregoryanz, O. Degtyareva, M. I. McMahon, M. Hanfland, S. Evans, M. Guthrie, S. V. Sinogeikin and H.-K. Mao, *Nat. Phys.*, 2011, **7**, 211–214.
159 M. Marqués, M. I. McMahon, E. Gregoryanz, M. Hanfland, C. L. Guillaume, C. J. Pickard, G. J. Ackland and R. J. Nelmes, *Phys. Rev. Lett.*, 2011, **106**, 095502.
160 M.-S. Miao and R. Hoffmann, *Acc. Chem. Res.*, 2014, **47**, 1311–1317.
161 H. Tang, B. Wan, B. Gao, Y. Muraba, Q. Qin, B. Yan, P. Chen, Q. Hu, D. Zhang, L. Wu, M. Wang, H. Xiao, H. Gou, F. Gao, H. Mao and H. Hosono, *Adv. Sci.*, 2018, **5**, 1800666.
162 Z. Zhao, S. Zhang, T. Yu, H. Xu, A. Bergara and G. Yang, *Phys. Rev. Lett.*, 2019, **122**, 097002.
163 B. Wan, S. Xu, X. Yuan, H. Tang, D. Huang, W. Zhou, L. Wu, J. Zhang and H. Gou, *J. Mater. Chem. A*, 2019, **7**, 16472–16478.
164 X. Zhong, M. Xu, L. Yang, X. Qu, L. Yang, M. Zhang, H. Liu and Y. Ma, *npj Comput. Mater.*, 2018, **4**, 70.
165 M. Miao, X. Wang, J. Brgoch, F. Spera, M. G. Jackson, G. Kresse and H. Lin, *J. Am. Chem. Soc.*, 2015, **137**, 14122–14128.
166 Q. Zhu, A. R. Oganov and A. O. Lyakhov, *Phys. Chem. Chem. Phys.*, 2013, **15**, 7696.
167 K. Horiba, R. Yukawa, T. Mitsuhashi, M. Kitamura, T. Inoshita, N. Hamada, S. Otani, N. Ohashi, S. Maki, J. Yamaura, H. Hosono, Y. Murakami and H. Kumigashira, *Phys. Rev. B*, 2017, **96**, 045101.
168 L. Pauling, *J. Am. Chem. Soc.*, 1933, **55**, 1895–1900.
169 N. Bartlett, *Proc. Chem. Soc. Lond.*, 1962, **6**, 197–236.
170 F. Peng, X. Song, C. Liu, Q. Li, M. Miao, C. Chen and Y. Ma, *Nat. Commun.*, 2020, **11**, 1–7.
171 J. Zhang, J. Lv, H. Li, X. Feng, C. Lu, S. A. T. Redfern, H. Liu, C. Chen and Y. Ma, *Phys. Rev. Lett.*, 2018, **121**, 255703.
172 J. Shi, W. Cui, J. Hao, M. Xu, X. Wang and Y. Li, *Nat. Commun.*, 2020, **11**, 3164.
173 Y. Bai, Z. Liu, J. Botana, D. Yan, H.-Q. Lin, J. Sun, C. J. Pickard, R. J. Needs and M.-S. Miao, *Commun. Chem.*, 2019, **2**, 102.
174 C. Liu, H. Gao, Y. Wang, R. J. Needs, C. J. Pickard, J. Sun, H.-T. Wang and D. Xing, *Nat. Phys.*, 2019, **15**, 1065–1070.
175 B. Monserrat, M. Martinez-Canales, R. J. Needs and C. J. Pickard, *Phys. Rev. Lett.*, 2018, **121**, 015301.
176 H. Gao, C. Liu, A. Hermann, R. J. Needs, C. J. Pickard, H.-T. Wang, D. Xing and J. Sun, *Natl. Sci. Rev.*, 2020, **7**, 1540–1547.
177 C. Liu, H. Gao, A. Hermann, Y. Wang, M. Miao, C. J. Pickard, R. J. Needs, H.-T. Wang, D. Xing and J. Sun, *Phys. Rev. X*, 2020, **10**, 021007.
178 F. Peng, Y. Wang, H. Wang, Y. Zhang and Y. Ma, *Phys. Rev. B: Condens. Matter Mater. Phys.*, 2015, **92**, 094104.
179 Z. Liu, J. Botana, M. Miao and D. Yan, *Europhys. Lett.*, 2017, **117**, 26002.
180 F. Peng, J. Botana, Y. Wang, Y. Ma and M. Miao, *J. Phys. Chem. Lett.*, 2016, **7**, 4562–4567.
181 C. Sanloup, S. A. Bonev, M. Hochlaf and H. E. Maynard-Casely, *Phys. Rev. Lett.*, 2013, **110**, 265501.

182 S. Zhang, H. Bi, S. Wei, J. Wang, Q. Li and Y. Ma, *J. Phys. Chem. C*, 2015, **119**, 24996–25002.
183 M. Somayazulu, P. Dera, A. F. Goncharov, S. A. Gramsch, P. Liermann, W. Yang, Z. Liu, H. Mao and R. J. Hemley, *Nat. Chem.*, 2010, **2**, 50–53.
184 M. Somayazulu, P. Dera, J. Smith and R. J. Hemley, *J. Chem. Phys.*, 2015, **142**, 104503.
185 X. Yan, Y. Chen, X. Kuang and S. Xiang, *J. Chem. Phys.*, 2015, **143**, 124310.
186 A. Dewaele, P. Loubeyre, P. Dumas and M. Mezouar, *Phys. Rev. B: Condens. Matter Mater. Phys.*, 2012, **86**, 014103.
187 D. Laniel, G. Weck and P. Loubeyre, *Phys. Rev. B*, 2016, **94**, 174109.
188 Z. Liu, J. Botana, A. Hermann, S. Valdez, E. Zurek, D. Yan, H. Lin and M. Miao, *Nat. Commun.*, 2018, **9**, 951.
189 T. Plisson, G. Weck and P. Loubeyre, *Phys. Rev. Lett.*, 2014, **113**, 025702.
190 G. Xiao, T. Geng and B. Zou, *ACS Mater. Lett.*, 2020, **2**, 1233–1239.
191 Y. Wang and Y. Ma, *J. Chem. Phys.*, 2014, **140**, 040901.
192 V. Vassilev-Galindo, G. Fonseca, I. Poltavsky and A. Tkatchenko, *J. Chem. Phys.*, 2021, **154**, 094119.
193 Y. A. Wang and E. A. Carter, in *Theoretical Methods in Condensed Phase Chemistry*, Kluwer Academic Publishers, Dordrecht, 2005, pp. 117–184.
194 R. Lopez de Mantaras and E. Armengol, *Data Knowl. Eng.*, 1998, **25**, 99–123.
195 W. WU and Q. SUN, *Sci. Sin. Phys. Mech. Astron.*, 2018, **48**, 107001.
196 J. Wei, X. Chu, X. Sun, K. Xu, H. Deng, J. Chen, Z. Wei and M. Lei, *InfoMat*, 2019, **1**, 338–358.
197 Q. Tong, L. Xue, J. Lv, Y. Wang and Y. Ma, *Faraday Discuss.*, 2018, **211**, 31–43.
198 Q. Tong, P. Gao, H. Liu, Y. Xie, J. Lv, Y. Wang and J. Zhao, *J. Phys. Chem. Lett.*, 2020, **11**, 8710–8720.
199 G. N. Simm, A. C. Vaucher and M. Reiher, *J. Phys. Chem. A*, 2019, **123**, 385–399.
200 M. B. Smith, *March's advanced organic chemistry: reactions, mechanisms, and structure*. John Wiley & Sons, 2020.